Study of Multilayer Treatments of Nitrocarburizing with N and Si-doped DLC Films in Improving the Wear Resistance of AISI M2 Steel

M.R. Danelon[a]* , L.S. Almeida[b] , E.C.T Ba[c] ,

P.S. Martins[d] , M. D. Manfrinato[e] , L.S. Rossino[b,e]

[a]Universidade de São Paulo (USP), Escola Politécnica, Departamento de Engenharia Metalúrgica e de Materiais, São Paulo, SP, Brasil.
[b]Universidade Federal de São Carlos (UFSCar), Sorocaba, SP, Brasil.
[c]Universidade Federal de Uberlândia (UFU), Uberlândia, MG, Brasil.
[d]Pontifícia Universidade Católica de Minas Gerais (PUC), Belo Horizonte, MG, Brasil.
[e]Faculdade de Tecnologia de Sorocaba (FATEC-So), Sorocaba, SP, Brasil.

Diamond-like Carbon (DLC) films demonstrate substantial hardness, minimal friction, and exceptional wear resistance when applied to metal substrates; however, they face challenges related to inadequate adhesion. Furthermore, concerns about thermal stability are prevalent in DLC films, particularly concerning cutting tools, where processing temperatures may reach significant levels. To mitigate these issues, incorporating various dopants and applying multilayer treatments may enhance adhesion, thermal stability, and wear resistance while simultaneously decreasing the coefficient of friction. This study systematically examines the effects of nitrogen and silicon doping on DLC films applied to M2 steel. It employs multilayer treatments to evaluate their influence on wear resistance, employing a fixed ball wear test that monitors wear progression by interrupting the test at various intervals. Plasma treatments, including nitriding, nitrocarburizing, and DLC coatings, were evaluated independently and in combination. A combination of DLC coatings with nitrocarburizing proved to be better for wear resistance when both the coating and the compound layer present a controlled thickness and high hardness, promoting low friction and avoiding debris formation. The findings reveal that Si-doped DLC combined with nitrocarburized layers significantly improves wear resistance and adhesion, highlighting the benefits of integrating duplex treatments with DLC doping to enhance coating performance.

Keywords: *Doped DLC Film, Tool Steel, Coatings, Nitrocarburizing, Wear Tests.*

1. Introduction

DLC films, also known as diamond-like carbon films, are classified as amorphous carbon films characterized by both sp^2 and sp^3 carbon-carbon hybridizations. These hybridizations are closely associated with the properties found in graphite and diamond[1]. The resulting structure endows these films with exceptional hardness, a low coefficient of friction, and outstanding wear resistance. Nonetheless, the adhesion properties of these films on metallic surfaces present a considerable challenge, attributed to the significant disparity in hardness and thermal expansion coefficients between the films and their respective substrates[2]. In response to this challenge, several alternative approaches have been proposed, including the incorporation of an organosilicon interlayer[2-4], the application of duplex coatings[5-7], and the doping of the DLC films with various elemental constituents[8-10].

The primary referenced alternative does not directly improve the characteristics of the Diamond-Like Carbon (DLC); nevertheless, it does contribute to the enhancement of the film's tribological behavior, as its function is to mitigate internal stresses and promote a uniform modification of the film's coefficient of thermal expansion[11].

Doping amorphous carbon films with various elements and applying duplex coatings can significantly enhance not only the adhesion of the film to the substrate but also its wear resistance performance[4,6,12]. Sharifahmadian et al.[10] investigated the doping of the DLC film with nitrogen, concluding that this process improves adhesion by facilitating the transformation of C-C sp^3 hybridizations into sp^2 hybridizations. In contrast, other studies suggest that the presence of nitrogen within the film may also augment wear resistance in comparison to the undoped film, albeit with a concomitant reduction in the hardness of these films[8,10,13,14].

The incorporation of silicon in diamond-like carbon (DLC) films significantly enhances their tribological performance and mechanical characteristics, attributed to the stabilization of sp^3 hybridizations at elevated temperatures[15]. This property holds potential relevance for applications in cutting tools, which necessitate superior performance under high thermal

*e-mail: miguel.danelon@usp.br

conditions. Regarding the tribological behavior and mechanical properties of these films, certain discrepancies in the findings have been documented. Notably, the wear resistance of silicon-doped DLC films may surpass that of conventional DLC films, as demonstrated by Kim et al.[16], wherein the wear rate and hardness of silicon-doped DLC films were found to be lower than those of conventional counterparts. Conversely, research by Vengudusamy et al.[17] suggests that under dry conditions, silicon-doped DLC films exhibited a reduced wear rate and an increased hardness relative to conventional DLC films.

As previously indicated, duplex treatments serve as an alternative that can improve the adhesion properties of Diamond-Like Carbon (DLC) films on metallic substrates and enhance their mechanical characteristics and performance[18,19]. The duplex treatment effectively mitigates the cohesive and adhesive failures typically observed in conventional DLC deposition by accommodating the substrates' plastic deformation[7].

This feature possesses the potential to positively influence the tribological behavior of materials subjected to duplex treatment, as elucidated by Dalibon et al.[20], Danelon et al.[6], and Yetim et al.[21]. Their investigations demonstrated that the duplex treatment, which involves nitriding combined with a DLC film, enhances the wear resistance of metals. These findings can be rationalized by the enhancement of the film's adhesion properties through mechanical interlocking facilitated by the roughness of the nitriding compound layer. Moreover, the formation of a gradient of properties between the coatings and the substrate occurs abruptly when exclusively employing the conventional DLC film with an interlayer[22-25].

While numerous studies have examined both the doping of Diamond-Like Carbon (DLC) films and the application of duplex treatments, there exists a paucity of literature that concurrently investigates these conditions to assess their impact on the wear performance of the materials. Furthermore, even fewer studies have addressed these treatments specifically in relation to high-speed steels.

This study examines the impact of duplex treatments involving nitrocarburizing with varying concentrations of diamond-like carbon films on the tribological performance of AISI M2 steel and compares these findings to those of the individual treatments of nitriding, nitrocarburizing, DLC, nitrogen-doped DLC, and silicon-doped DLC.

2. Material and Methods

AISI M2 tool steel substrates were sectioned into specimens measuring 10x10x13 mm and subjected to a quenching process at a temperature of 1050 °C. Subsequently, the specimens were cooled in oil at 80 °C and tempered at 550 °C for two hours. Following the heat treatment process, the specimens underwent grinding using #220, #320, #400, #600, #1200, and #2500 mesh sandpaper. Furthermore, they were polished with a diamond paste featuring an abrasive particle size of 3 μm and subsequently cleaned using ultrasonic cleaning equipment with ethanol for 10 minutes.

Thermochemical treatments and thin film depositions were conducted utilizing plasma treatment and Plasma Enhanced Chemical Vapor Deposition (PECVD) techniques, respectively, employing a pulsed-DC power supply situated at LabTES (Surface Treatment and Engineering Laboratory). Prior to each treatment, a plasma ablation cleaning process was executed with a gas mixture comprising 80% Argon and 20% Hydrogen for one hour at a pressure of 2 torr, maintained at the temperature designated for the subsequent thermochemical treatment or film deposition.

Table 1 presents the simplified treatment parameters. Thermochemical treatments of nitriding and nitrocarburizing were conducted utilizing a gas flow rate of 750 standard cubic centimeters per minute (sccm) at a pressure of 2.8 torr. The thin film depositions, specifically diamond-like carbon (DLC), nitrogen-doped DLC (N-DLC), and silicon-doped DLC (Si-DLC), were executed with a total gas flow of 30 sccm and a voltage of 500 V at a pressure of 0.09 torr. Prior to the deposition of the DLC film, an organosilicon interlayer was applied using hexamethyldisiloxane (HMDSO) as the precursor at a pressure of 0.25 torr.

Typically, when doping diamond-like carbon (DLC) films with silicon, the precursor used is silane (SiH_4)[26]. Silane is a gas similar to methane; however, it is pyrophoric and flammable under pressure, which poses a security risk in industrial and laboratory settings. Alternatively, highly volatile liquids such as hexamethyldisiloxane (HMDSO) may be employed, which is non-flammable, non-toxic, and more cost-effective than silane[27]. Its remarkable ability to form covalent bonds between organic and inorganic compounds, along with the stability of the Si-O-Si bond, enhances the potential of utilizing this component in high-performance coatings[27,28].

In the case of multilayer treatments, a combination of nitrocarburizing (NITC) with various types of diamond-like carbon (DLC) films, based on the doping elements, was produced utilizing the same parameters as delineated in Table 1. Consequently, the nomenclature of the multilayer treatments is designated as NITC+DLC, NITC+N-DLC, and NITC+Si-DLC for the deposition of DLC, N-DLC, and Si-DLC films, respectively. Figure 1 illustrates the

Table 1. Treatment parameters for the simple treatment condition.

	Treatment	Gas mixture (%)	Time (h)	Temperature (°C)	Nomenclature
	Nitriding	$80N_2$-$20H_2$	6	450	NIT
	Nitrocarburizing	$80N_2$-$15H_2$-$5CH_4$	6	450	NITC
DLC	Organosilicon interlayer	70HMDSO-30Ar	0.25		DLC
	DLC film	$90CH_4$-10Ar	2		
N-DLC	Organosilicon interlayer	70HMDSO-30Ar	0.25	300	N-DLC
	N-DLC film	$70CH_4$-$30N_2$	2		
Si-DLC	Organosilicon interlayer	70HMDSO-30Ar	0.25		Si-DLC
	Si-DLC film	$90CH_4$-8Ar-2HMDSO	2		

schematization of the treatments, indicating the sequential steps involved in the multilayer treatments.

Subsequent to the treatments, metallographic analyses were conducted on the cross-sections of samples embedded in Bakelite. These samples were subjected to grinding using #220, #320, #400, #600, #1200, and #2500 mesh sandpaper, followed by polishing with a three μm diamond paste and chemical etching using Nital 3%. Micrography analysis was performed utilizing a Hitachi TM-3000 Scanning Electron Microscope (SEM) configured for backscattered signal detection at 15 kV. Furthermore, a semi-quantitative chemical analysis was executed through Electron Dispersive Spectroscopy (EDS) to ascertain the elemental composition present in the layers and films produced during the thermochemical treatments and diamond-like carbon (DLC) depositions. Furthermore, Raman spectroscopy was utilized to examine the structural properties of both doped and undoped diamond-like carbon (DLC). This analysis was conducted using an argon laser operating at a wavelength of 513 nm, which constituted 5% of the overall power of the equipment. It employed a laser spot with a diameter of 5 μm. The analyses were executed using a Renishaw Via Raman Microscope, and the spectral data were processed utilizing Fityk version 0.9.8 software, focusing on the deconvolution of G and D bands to ascertain the specific parameters obtained from the analysis films.

Equation 1 was utilized to ascertain the theoretical hydrogen content within the undoped diamond-like carbon (DLC) film[29]. Additionally, Equation 2 was employed to evaluate the sp^3 content within the films[30].

$$H\left[at\ \%\right] = 21.7 + 16.6 loglog\left(\frac{m}{I(G)}\right)\left[\mu m\right] \tag{1}$$

$$sp^3\ content = 0.24 - 48.9\left(Pos(G) - 0.1580\right) \tag{2}$$

where m represents the slope of the spectrum ranging from 1000 to 1800 cm-1, I(G) denotes the intensity of the G band, and Pos (G) indicates the position of the G band measured in μm-1.

In addition to the primary analysis, a Fourier Transform Infrared (FTIR) spectroscopy was conducted to determine the bonding characteristics of both doped and undoped diamond-like carbon (DLC) films. The analyses were carried out using the Jasko FTIR-410 spectrometer, employing a scanning frequency of 128 seconds at a resolution of 4 cm^{-1}.

In order to characterize the mechanical properties of the layers produced through nitriding and nitrocarburizing treatments, as well as the deposited interlayer and DLC films, microhardness tests were conducted in accordance with the ASTM E348-99 standard. The Mitutoyo HM220 digital microhardness tester was employed, utilizing a load of 0.1 kgf for superficial hardness and a load of 0.01 kgf for profile hardness. These tests were performed on the cross-section of samples exhibiting both compound layers and diffusion zones, with a duration of 15 seconds for all assessments.

Adhesion tests were conducted in the Diamond-Like Carbon (DLC) films in accordance with the VDI 3198 standard[31]. This process involved executing a Rockwell C test on the surface of the films and examining the characteristics of the resulting indentation. The Rockwell C tests were performed utilizing a Mitutoyo hardness tester HR 300. The indentation generated on the film surface was captured using a Hitachi TM-3000 Scanning Electron Microscope (SEM) and analyzed through ImageJ to assess the adhesion area of the film quantitatively.
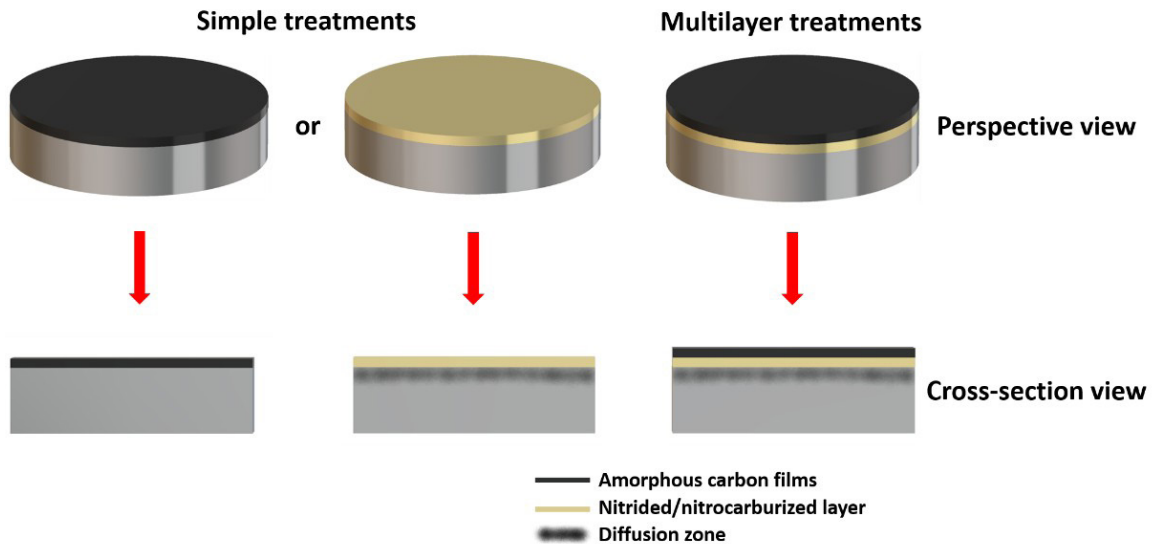

Figure 1. Schematization of the simple and multilayer treatment development.

The samples were characterized by a fixed ball wear test employing an AISI 52100 sphere as the counter-body, with a load of 8 N, a rotation frequency of 158 rpm, and sliding distances of 31.5 m (2 minutes), 63.1 m (5 minutes), 126.1 m (10 minutes), 189.1 m (15 minutes), 252.2 m (20 minutes), 315.2 m (25 minutes), and 378.2 m (30 minutes). The tests were conducted using a crater-over-crater methodology, indicating that subsequent sliding distances were performed at the exact location of the previous crater. The craters were analyzed and measured utilizing a portable stereoscope, and the wear volume (V) was calculated in accordance with Equation 3, which is essential for assessing the wear resistance of both treated and untreated materials[32].

$$V = \frac{\pi b^4}{64R} \quad to \ b <<< R \tag{3}$$

Where b represents the crater diameter, and R denotes the sphere utilized as the counter-body, it can be observed that a smaller crater diameter correlates with a reduced wear volume and, consequently, a higher wear resistance of the material[33].

The depth of the crater (H) was determined utilizing Equation 4 for comparison with the thickness of the deposited

films and surface layers produced following the tests. In this equation, V represents the wear volume, and R denotes the radius of the sphere employed as the counter-body[32].

$$H = \sqrt{\frac{V}{\pi R}} \tag{4}$$

3. Results and Discussion

Figure 2 illustrates the micrography of the cross-section of samples subjected to both simple and multilayer treatments. In Figure 2 A), the NITC sample cross-section exhibits a compound layer measuring 2.15 μm, whereas the NIT sample develops a compound layer of 3.11 μm. Notably, the NITC layer is thinner than the NIT compound layer, a result that can be elucidated through two primary explanations. According to Gonzalez-Carmona et al.[34], the affinity of carbon for certain elements that possess insufficient electrons in their d orbitals, such as Chromium (Cr), Tungsten (W), and Molybdenum (Mo), the alloying elements of AISI M2 steel, facilitates their bonding, resulting in the formation of carbides as opposed to nitrocarbides, thereby diminishing the thickness of the compound layer. Furthermore, the
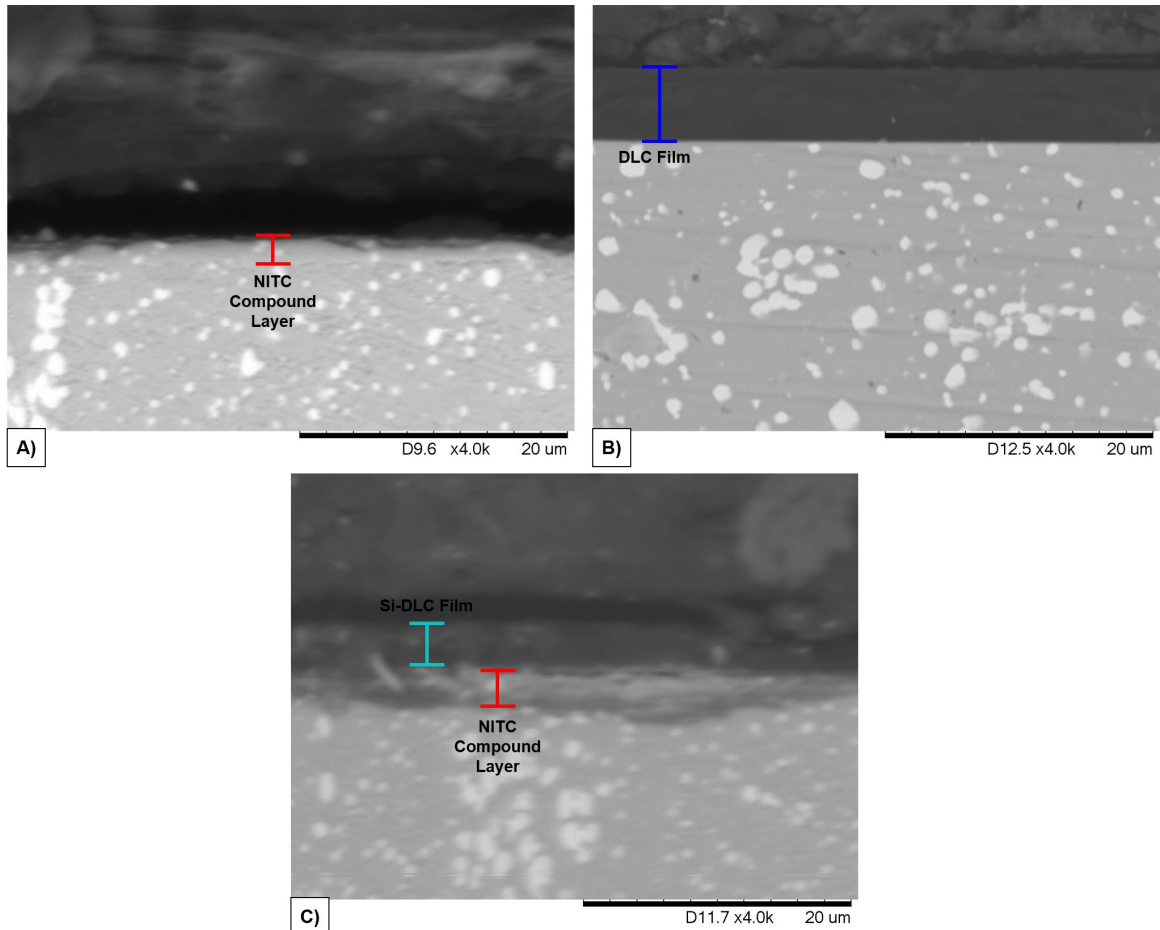
Figure 2. Micrography of the produced coatings in A) NITC, B) DLC, and H) NITC+Si-DLC by SEM with 4000x magnification.

ionization of CH_4 necessitates less energy than that of N_2, thus contributing to enhanced diffusion of carbon during plasma treatments. This increased carbon diffusion signifies that carbon will penetrate the matrix rather than remain concentrated within the compound layer, consequently leading to a reduction in its thickness while augmenting the thickness of the diffusion zone[35].

Figure 2B) illustrates the cross-section of the Diamond-Like Carbon (DLC) sample, which exhibits the most significant thickness among the films, measuring 5.51 μm. Conversely, the nitrogen-doped DLC (N-DLC) demonstrates the thinnest layer at a thickness of 3.05 μm. This reduction in thickness attributable to nitrogen doping has been noted previously by Almeida et al.[3]. This phenomenon can be elucidated by the sputtering effect caused by nitrogen atoms, which remove carbon atoms from the film's surface during layer deposition, thereby decreasing the deposition rate. Additionally, the evaporation of N_2 molecules occurs due to the recombination of N-N bonds. Such behavior is anticipated in nitrogen-doped DLC, as nitrogen evaporation from the film increases with the rising natural disorder during film formation[36]. The silicon-doped DLC (Si-DLC) film exhibits an intermediary thickness when compared to the N-DLC and DLC films, with a recorded thickness of 4.32 μm.

Figure 2C) illustrates the cross-section of the NITC+Si-DLC sample, wherein the red line and cyan line denote the compound layer and the Si-DLC film, respectively. The thickness of the compound layer, attributed to the nitrocarburizing treatment, measures 3.33 μm, while the deposited Si-DLC film exhibits a thickness of 3.40 μm. It is essential to emphasize that the thickness of the Si-DLC film decreased during the multilayer treatment in comparison to the simple treatment, which recorded a thickness of 4.32 μm.

The observed reduction in thickness may be attributed to the diffusion of carbon into the nitrocarburized compound layers, as noted by Danelon et al.[6] through XRD analyses of multilayer treatments, which revealed the presence of carbonitrides ε'. As carbon diffuses into the layers, it contributes to a reduction in the overall film thickness[6].

The chemical analysis of the elements observed in the DLC and N-DLC films (see Figure 3A) and Figure 3B), respectively) indicates an increase in silicon concentration between the film and the substrate due to the presence of the organosilicon interlayer in this region. Furthermore, the significant presence of carbon in the film evidences the formation of the carbon film. However, upon examining Figure 3C), which represents the Si-DLC, it is apparent that silicon levels are elevated throughout the entire film, attributable to silicon doping. Regarding the absence of nitrogen evidence depicted in Figure 3B), this is associated with the employed technique, as Energy Dispersive Spectroscopy (EDS) is not recommended for elements of low atomic number, particularly nitrogen, due to its K shell not being the valence shell[37].

The incorporation of silicon and nitrogen as a result of the doping film can be interpreted through the examination of the films' structural properties, specifically the structural alterations they entail in the coatings. One of the most significant techniques for characterizing carbon materials is Raman spectroscopy, which is illustrated in Figure 4.

Upon reviewing Figure 4A), it is evident that the Raman spectra of DLC, N-DLC, and Si-DLC closely resemble those documented in the literature[3,36,38]. The G band peak, located at 1550 cm^{-1}, corresponds to the vibrations of carbon with sp^2 hybridizations, indicating that this band is associated with the graphitic characteristics of DLC films. Conversely, the D band peak at 1355 cm^{-1} is linked to the structural disorder within the film, as indicated by the vibrations of sp^2 hybridized carbons in aromatic rings, mainly due to the presence of sp^3 hybridizations[2]. These two bands in the Raman shifts are characteristic of amorphous hydrogenated
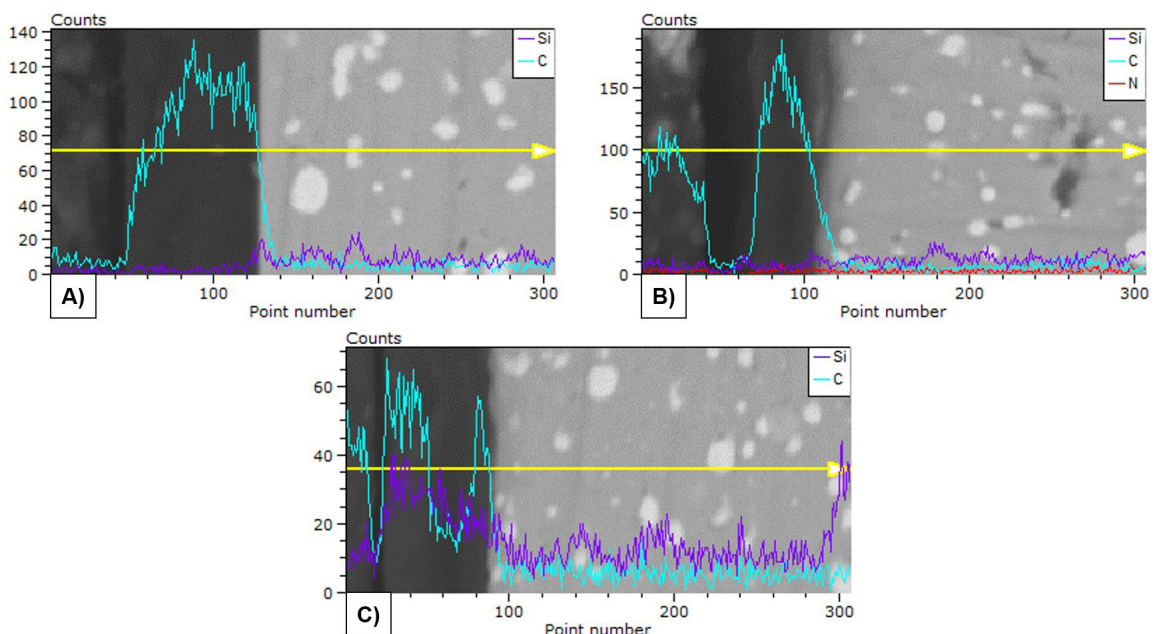
Figure 3. Chemical analysis of the elements determined by EDS via MEV using line mode A) DLC, B) N-DLC, and C) Si-DLC samples.

carbon (a:C-H), signifying that these films are amorphous, attributable to the disorder and the varying types of carbon bonding, which confer properties that bridge the gap between graphite and diamond. The investigation of DLC utilizing Raman spectroscopy can be conducted by analyzing the intensity ratio of the D and G bands (I_D/I_G), the position of the G band, and its full width at half maximum (FWHM)[39]. The content of sp[3] hybridization, for instance, can be estimated by situating these findings within the graphite amorphization trajectory as presented by Ferrari and Robertson[39].

By analyzing the intensities—where the area of these bands is relevant—of the G and D bands for each film, it is possible to determine the I_D/I_G ratio, which reflects variations in sp[3] hybridizations within the film. A decrease in the I_D/I_G ratio indicates an inability for aromatic rings to form, thereby increasing the disorder of the film. This observation suggests that the material contains a greater quantity of sp[3] carbons in comparison to a film exhibiting a higher I_D/I_G ratio. Table 2 presents the I_D/I_G ratios for DLC, N-DLC, and Si-DLC films derived from the area analysis of each respective band.

The I_D/I_G ratio of the nitrogen-doped diamond-like carbon (N-DLC) sample exhibits the highest value compared to the other films. The transformations of sp[3] can elucidate this phenomenon to sp[2] hybridizations induced by nitrogen doping in the film. This process enhances the stability of aromatic rings, consequently sustaining a more significant proportion of sp[2] hybridizations.

In contrast to this outcome, the Si-DLC demonstrated the lowest I_D/I_G ratio when compared to the other films. According to Cemin et al.[40], a decrease in the intensities ratio of the D and G bands indicates a more significant presence of sp[3] hybridizations. This finding is consistent with those reported by Wu and Hon[15] which associate silicon doping with the stabilization of sp[3] hybridizations in Si-DLC films.

The presence of silicon (Si) reduces the I_D/I_G ratio, as its incorporation diminishes the size of the sp[2] cluster through the opening of sp[2] rings. This phenomenon occurs due to the inability of Si atoms to form π bonds, which consequently lowers the ratio, signifying an increase in the presence of sp[3] hybridizations[41].

As indicated by Equation 1, a significant structural parameter that can be derived from Raman spectroscopy is the percentage of hydrogen present in the film. Casiraghi et al.[29] observe that the incorporation of hydrogen into the chemical composition of amorphous carbon facilitates the differentiation of sp[3] hybridizations into C-C and C-H sp[3] bonds, thereby altering the connectivity of sp[3] bonds and the configurations of sp[2] clusters. The diamond-like carbon (DLC) film exhibits a hydrogen content of 36.39% (as presented in Table 2), which, as noted by Robertson[1], classifies this film as an amorphous carbon-hydrogen (a:C-H) hard DLC film, typically produced through plasma-enhanced chemical vapor deposition (PECVD) technique, given that the carbon source is derived from hydrocarbon gases. However, this method, as stipulated by Equation 1, is constrained to DLC films that are devoid of doping with various elements, as the presence of different components may interfere with the outcomes suggested by the equation above[1,29,42].

Utilizing Equation 2, it was feasible to ascertain the sp[3] content of these films, as illustrated in Table 2. As documented in the existing literature, a linear correlation exists between the displacement of the G band position and the sp[3] content, which corroborates the findings associated with the ID/IG ratio. Specifically, the DLC, N-DLC, and Si-DLC exhibited
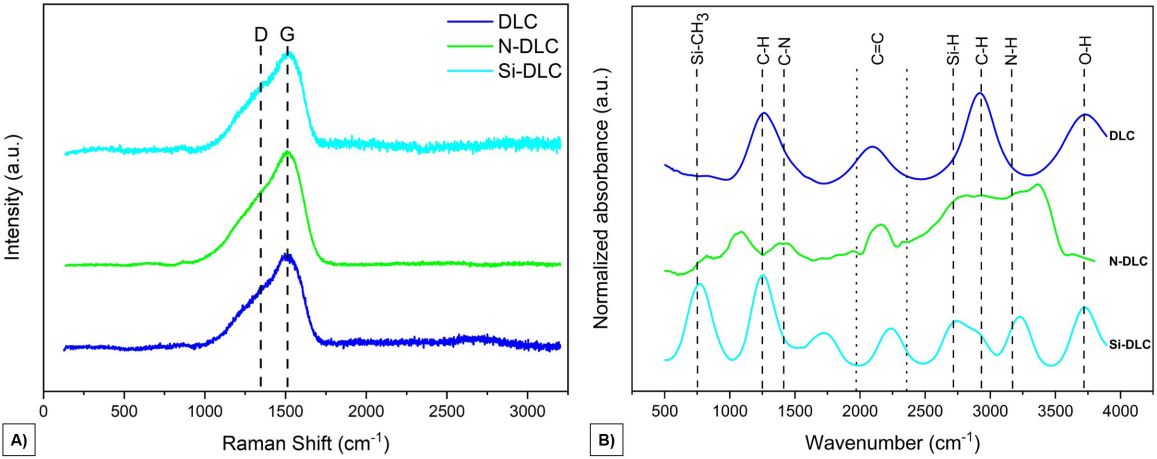
Figure 4. Structural analysis of the DLC, N-DLC, and Si-DLC films by A) Raman spectroscopy and C) FTIR spectroscopy.

Table 2. Parameters of Position of G and D band, FWHM of G band, I_D/I_G ratio, and theoretical hydrogen content of DLC, N-DLC, and Si-DLC films.

Sample	Pos (G) (cm⁻¹)	Pos (D) (cm⁻¹)	FWHM (G) (cm⁻¹)	I_D/I_G ratio	Hydrogen (%)	sp³ content
DLC	1512	1302	178	0.51	36,39	0.57
N-DLC	1522	1320	146	0.71	-	0.52
Si-DLC	1495	1265	292	0.22	-	0.66

sp^3 contents of 0.57, 0.52, and 0.66, respectively. Once again, the Si-doped DLC film demonstrated a higher sp^3 content, while the N-DLC exhibited lower sp^3 content when compared to the conventional DLC film. According to the research conducted by Ferrari and Robertson[39], the observed increase in the G position (indicative of lower sp^3 content) results from sp^2 groups characterized by a higher vibrational frequency due to the resonant selection of wider-band gap π[30,39].

The Full Width at Half Maximum (FWHM) of the films, as delineated in Table 2, demonstrates a correlation with the sp^3 content, indicating that an increase in FWHM corresponds to an elevated sp^3 content in the films. Furthermore, Ba et al.[38] corroborated this observation; however, Cui et al.[42] indicated that this correlation is only applicable to hydrogenated diamond-like carbon (DLC) films with a low hydrogen content, revealing a non-linear relationship for amorphous carbon with hydrogen (a-C:H) films. The stress introduced by the incorporation of hydrogen into the films manifests as an increase in sp^3 content due to the presence of smaller cluster sizes while simultaneously exhibiting a decrease attributed to enhanced bonding with hydrogen atoms. This interplay elucidates why the FWHM (G) shows a weak correlation with the sp^3 content of the film[29,42].

Figure 4C) illustrates the FTIR spectroscopy of the DLC, N-DLC, and Si-DLC samples. Each sample exhibits absorption peaks at approximately 1250 and 2900 cm^{-1}, which can be attributed to the stretching of C-H bonds. Additionally, all samples displayed peaks within the range of 1970 to 2400 cm^{-1}, corresponding to the stretching of C=C bonds. At 3700 cm^{-1}, the samples exhibit peaks that may relate to O-H bonding. These peaks are characteristic of conventional amorphous carbon films[3,9,43].

Upon analyzing the Fourier Transform Infrared (FTIR) spectrum of the nitrogen-doped diamond-like carbon (N-DLC) sample, it is observable that peaks are present at 1700 cm^{-1} and 3200 cm^{-1}. These peaks can be ascribed to the stretching vibrations of C-H and N-H bonds, respectively. Their presence is a direct result of the nitrogen doping present in the film[3,44].

Similar behavior is observed in the Si-DLC peaks, where there exists a peak at 752 cm^{-1}, which is associated with the stretching of the $Si-CH_3$ bonding, originating from the presence of silicon within the film[9,15].

Figure 5A). presents the hardness profiles of NIT and NITC. These results are essential only for samples that went through nitriding or nitrocarburizing treatments since they show a diffusion zone.

In addition to these findings, Table 3 illustrates the superficial hardness and total thickness of the layers or films corresponding to each treatment.
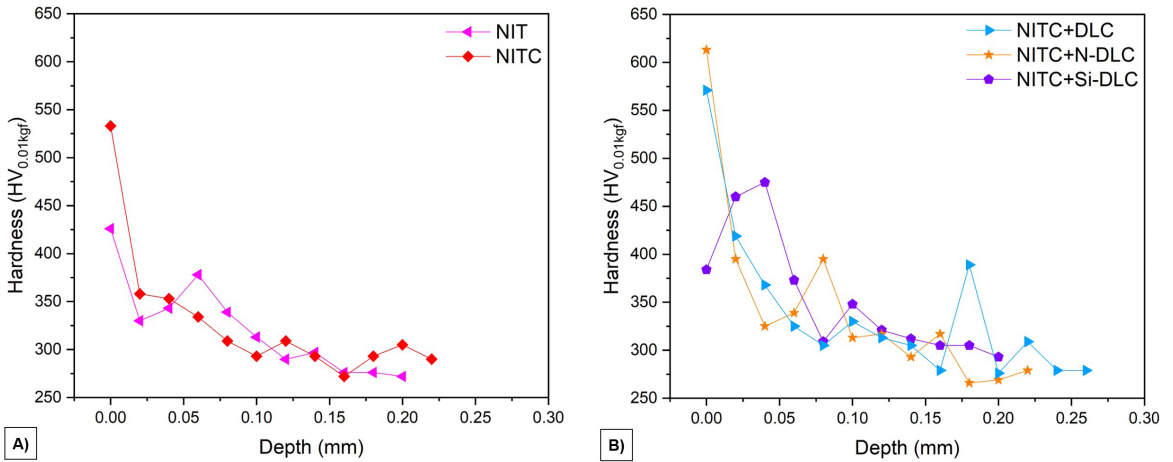
Figure 5. Vickers microhardness of the treatments A) NIT and NITC and B) NITC+DLC, NITC+N-DLC, and NITC+Si-DLC with a load of 0.01kgf.

Table 3. Superficial hardness and layer/film thickness of treatments.

Treatment	Superficial Hardness (HV$_{0.1kgf}$)	Layer thickness (μm)			
		Film	Compound Layer	Diffusion	Total
NIT	843 ± 18	-	3.11	180.00	183.11
NITC	955 ± 39	-	2.15	200.00	202.15
DLC	895 ± 39	5.51	-	-	5.51
N-DLC	849 ± 18	3.05	-	-	3.05
Si-DLC	981 ± 53	4.32	-	-	4.32
NITC+DLC	1676 ± 163	1.37	1.94	240.00	243.31
NITC+N-DLC	1757 ± 185	1.35	1.54	200.00	242.89
NITC+Si-DLC	1823 ± 78	3.40	3.33	180.00	183.33

In Figure 5A), it is possible to observe that NITC exhibits a slightly greater hardness at depth in comparison to NIT. This result can be attributed to the enhanced diffusion of carbon relative to nitrogen, as the hydrocarbon structures necessitate less energy for the decomposition of the CH_4 molecule during plasma treatments[35]. Furthermore, the initial hardness of the NIT sample is lower than that of the NITC sample, as the presence of carbon promotes the formation of ε' nitride, which possesses a hexagonal close-packed (HCP) crystalline structure that demonstrates greater hardness than γ' nitride, characterized by a face-centered cubic (FCC) crystalline structure, typical of nitriding treatment[45-47].

The hardness at the depths resulting from nitrocarburizing treatments on M2 steel, utilized as a substrate in this study, is inferior to that observed in treatments conducted on AISI 4340 steel by Campos et al.[4], wherein the depth of hardness achieved was 400 μm, in contrast to the 200 μm recorded in the present investigation. This reduction in hardness depth can be attributed to the variance in the types of steel employed. Specifically, in the case of AISI M2 steel, the alloying elements, namely chromium (Cr), vanadium (V), and tungsten (W), hinder the diffusion of elements through their reactive interactions. Moreover, the differing percentages of carbon between AISI M2 and AISI 4340 steels play a significant role in diminishing the depth of the diffusion zone, as carbon occupies interstitial sites within the steel and interacts with the alloying elements, thereby complicating the interaction of nitrogen with the matrix material[4,48,49]. A comparable hardness depth for AISI M2 steel was identified by Sousa et al.[50], which was approximately 200 μm.

The increased hardness of the NITC sample (955 HV) as compared to the NIT sample (843 HV) is elucidated by the same rationale presented in Figure 5A), wherein ε' nitrides exhibit a higher hardness than γ' nitrides due to variations in crystalline structure[45,51,52].

Upon analyzing the multilayer treatments NITC+DLC, NITC+N-DLC, and NITC+Si-DLC (illustrated in Figure 5B), the latter treatment exhibits the lowest hardness at varying depths among the multilayer treatments. This phenomenon can be attributed to the increased thickness of the nitrocarburized compound layer, which may diminish the nitrogen concentration within it, ultimately resulting in a reduction of hardness[53].

Furthermore, the diffusion zone of NITC+Si-DLC is shallower compared to that of NITC+DLC and NITC+N-DLC. This phenomenon may be attributable to the diffusion of carbon (C) and nitrogen (N) within the iron (Fe) matrix, as documented by Danelon et al.[6]. These elements possess small atomic radii, which facilitates interstitial diffusion. In contrast, silicon (Si) does not exhibit this behavior due to its relatively larger atomic radius, consequently leading to a reduced diffusion zone in treatments incorporating this element[6].

Upon analyzing the amorphous carbon films, it has been determined that the silicon-doped diamond-like carbon (Si-DLC) demonstrates a superior hardness value of 981 HV. This enhanced hardness is attributed to the stabilization of sp^3 hybridizations resulting from the incorporation of silicon into the film[15]. In contrast, the introduction of nitrogen as a dopant has resulted in a decrease in the hardness of the nitrogen-doped diamond-like carbon (N-DLC) sample, which records hardness values of 849 HV and 895 HV, respectively, when compared to the standard diamond-like carbon (DLC). This reduction in hardness is due to the transformation of sp^3 to sp^2 hybridizations occurring in relation to the proportion of nitrogen integrated into the DLC structure[10].

In the analysis of the deposited films on the multilayer treatments, it is observed that the superficial hardness is nearly double that of films deposited using simple treatments. This finding underscores the significance of employing multilayer treatment, which illustrates the synergy between the nitrocarburized compound layer and the DLC, N-DLC, and Si-DLC films. Such behavior enhances the mechanical properties of the bulk material, as documented by Danelon et al.[6].

It is essential to acknowledge that Vickers hardness is not the most appropriate method for assessing amorphous carbon thin films due to the influence of the substrate on the hardness results. Nevertheless, given that this method is the most suitable for nitrided compound layers, every measurement was conducted using Vickers microhardness for comparative purposes[54,55].
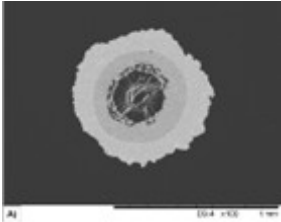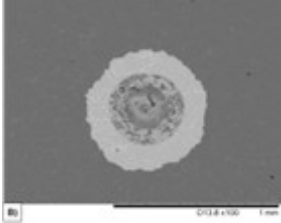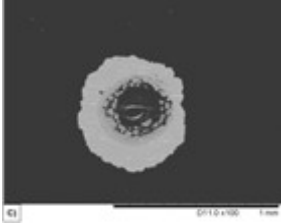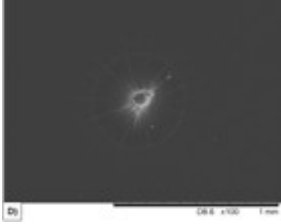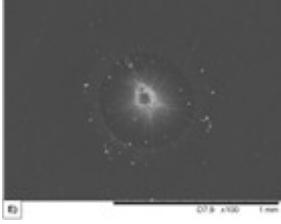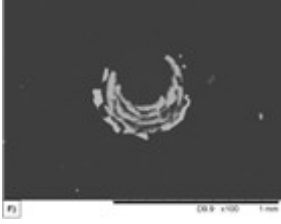
In the research conducted by Martins et al.[56], the nanoindentation technique was employed to assess the hardness and elastic modulus properties of an a-C:H diamond-like carbon (DLC) film. The results revealed that the surface hardness of the DLC measures 9.25 ± 2.10 GPa, which is, as anticipated, significantly higher than the hardness of AISI M35, recorded at 6.79 ± 0.51 GPa. Furthermore, the incorporation of diamond-like carbon within the coating's structure has substantially contributed to its hardness[56].

Table 4 illustrates the outcomes of the VDI 3189 adhesion test conducted on samples exhibiting amorphous carbon films on their surfaces. It is noteworthy to mention that none of the uncomplicated treatments applied to the amorphous carbon films achieved acceptable adhesion standards as per the VDI 3189 criteria, with DLC, N-DLC, and Si-DLC categorized as HF6, HF5, and HF5, respectively.

According to the authors' hypothesis, this behavior can be explained by the interaction of the film with the AISI M2 substrate. Although an organosilicon interlayer exists between the substrate and the film to mitigate the disparity in expansion coefficients and the significant difference in hardness between the two, the substrate exhibits precipitates that could adversely affect the adhesion of the film to the substrate. Therefore, a thin silicon-based interlayer is insufficient to ensure acceptable adhesion of the amorphous carbon films on the AISI M2 substrate despite the inclusion of nitrogen and silicon doping.

In their evaluation of the tribological behavior of the a-C:H diamond-like carbon (DLC) film deposited on high-speed steel AISI M2, Martins et al.[56] report commendable adhesion of the coatings on surfaces characterized by both gross and polished finishes, with minimal detachment of the film occurring, and no observable fractures around the indentation marks, thereby categorizing it as HF2. Conversely, the ground substrate displayed inadequate adhesion of the film, evidenced by significant detachment surrounding the indentation, leading to the characterization of the failure of the coating as HF5. Nevertheless, the authors concluded that this observed result did not constitute a decisive factor influencing the wear behavior of the coating, as it exhibited superior wear resistance despite poor adhesion.

Table 4. Results of the adhesion test of sample A) DLC, B) N-DLC, C) Si-DLC, D) NITC+DLC, E) NITC+N-DLC, and F) NITC+Si-DLC according to VDI 3189 standard.

Sample	Adhesion test	Classification	Delaminated area (%)
DLC		HF6	95.9
N-DLC		HF5	95.0
Si-DLC		HF5	95.6
NITC+DLC		HF1	22.97
NITC+N-DLC		HF1	23.78
NITC+Si-DLC		HF2	89.5

In contrast to the amorphous carbon films deposited through simple treatments, those deposited via multilayer treatments exhibited satisfactory adhesion properties for DLC, N-DLC, and Si-DLC, classified respectively as HF1, HF1, and HF2. This behavior can be attributed to the synergy between the amorphous carbon films and the nitrocarburized compound layer, which enhances not only the corrosion and wear resistance of the bulk material but also the adhesion of thin films to the substrates. According to the findings of Ebrahimi et al.[18], the improved adhesion is associated with the mechanical locking adhesion mechanism facilitated by the roughness of the nitrocarburized surface, thereby promoting the anchoring of the film onto the surface.

Figure 6 presents the wear volume as a function of the sliding distances performed during the tests.

It is observed that all simple treatments exhibited a lower wear volume in comparison to the base material, thereby indicating the tribological efficiency of these treatments. Among these, the sample NIT demonstrated the least wear resistance due to its lower hardness relative to the other treatments, as illustrated in Table 3. When comparing the wear resistance of NIT with that of NITC, it is evident that NITC possesses superior wear resistance attributable to its higher hardness, a thinner and more uniform compound layer, along a diffusion zone that can effectively contain wear at a greater depth in contrast to the NIT sample. This observation is further supported by the findings of Danelon et al.[57], which suggest that the nitriding treatment results in enhanced wear resistance.

It is essential to clarify that a greater hardness of a compound layer does not invariably result in enhanced wear resistance. Instead, it is the interplay of various properties of the compound layer, including thickness, uniformity, and hardness, that determines its effectiveness. Thus, a compound layer's hardness alone cannot adequately justify an increase in wear resistance[57].

Upon analyzing DLC, N-DLC, and Si-DLC, it is observed that N-DLC exhibits the least wear resistance among the three variants, attributable to its reduced thickness and hardness when juxtaposed with DLC and Si-DLC. In contrast to the compound layers, the DLC films demonstrate superior wear resistance when characterized by increased thickness, as a greater sliding distance is required to degrade the film entirely[58].

Upon careful analysis of the DLC film exclusively, it is evident that it exhibits superior wear resistance, as evidenced by the lowest recorded wear volume in comparison to alternative samples. This observation holds even when juxtaposed with the multilayer treatments of NIC+DLC, NITC+N-DLC, and NITC+Si-DLC, evaluated up to a sliding distance of 252.15 meters. This remarkable performance can be attributed to its high hardness, substantial thickness, and low coefficient of friction contributed by the tribofilm that formed during the testing process.

In the comparative analysis of conventional DLC films and Si-DLC, it was observed that the DLC exhibited superior wear resistance up to a sliding distance of 378.23 meters. At this point, Si-DLC demonstrated a marginally lower wear volume of 2.78 x 10^{-4} m^3 compared to 2.82 x 10^{-4} m^3 for the conventional DLC film. It is noteworthy that despite a reduced thickness, the Si-DLC film achieved a wear volume comparable to that of the DLC film. This phenomenon can be attributed to silicon doping, which mitigates potential structural transformations within the amorphous carbon film at elevated temperatures that might adversely affect the tribological properties of the coating. Furthermore, silicon serves to stabilize the sp^3 hybridizations, effectively preventing the graphitization of the film and enhancing the hardness of the film at higher temperatures. Consequently, this improvement contributes to the wear resistance of the film over extended sliding distances[15,59].

It is noteworthy to observe that each DLC film exhibited superior wear resistance in comparison to NIT and NITC treatments. The formation of compound layers generates debris during testing, which has the potential to detach from the layer's surface and act in an abrasive manner, thereby exacerbating the wear resistance of these treatments. Furthermore, it is well-established that amorphous carbon films possess a lower coefficient of friction when contrasted with compound layers. When considering the additional properties of these films, this may elucidate the reduced wear volume of DLC films[60-63].

At a final sliding distance of 378.23 meters, the multilayer treatments of NITC+DLC and NITC+Si-DLC exhibited superior wear resistance when compared to other samples. This observation can be attributed to the enhanced adhesion provided by the multilayer treatments, resulting from the high hardness and low coefficient of friction characteristics of the DLC and Si-DLC on the surface. Furthermore, the hardness achieved at depth, attributed to the nitrocarburized layer, acts synergistically to enhance the wear resistance of the materials[6,63].
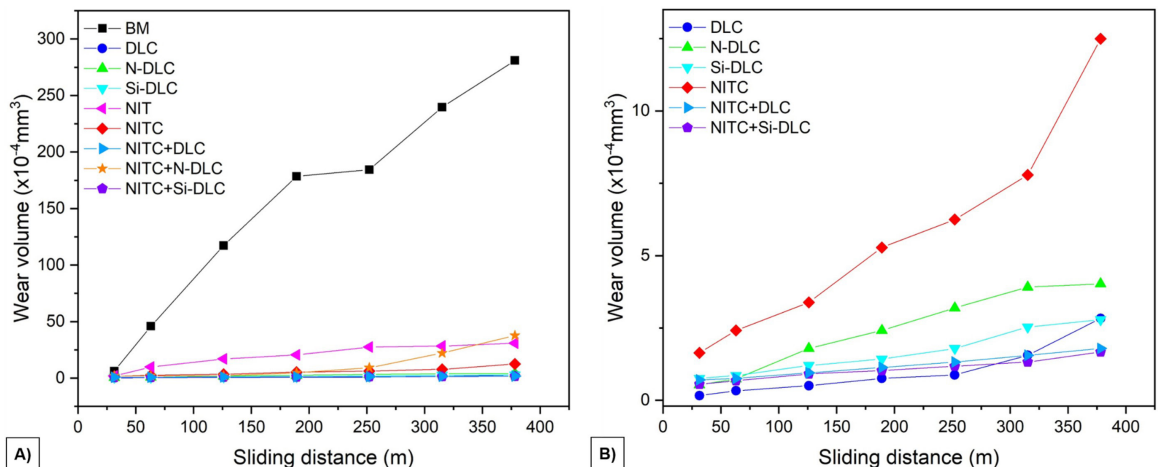

Figure 6. Wear volume as a function of the sliding distance obtained for the simple and multilayer treatments, A) complete graph and B) zoom in for lower wear volumes.

While the NITC+DLC and NITC+Si-DLC exhibited superior wear resistance among all tested samples at the conclusion of the sliding distance, the NITC+N-DLC demonstrated the highest wear volume among the treated specimens, surpassing only the base material. This phenomenon can be attributed to the reduced thickness of the N-DLC film, which may have experienced rapid wear, potentially resulting in the formation of debris released both from the film and the underlying nitrocarburized compound layer. This situation contributes to an increased wear volume for this specific sample[64,65].

A significant aspect worthy of analysis concerning the samples containing the Si-DLC, whether subjected to simple treatment (Si-DLC) or multilayer treatment (NITC+Si-DLC), is the consistent wear behavior observed across varying sliding distances, characterized by the absence of abrupt increments in wear volume. This consistency allows for an extension of the sliding distance while the wear volume of the sample continues to increase gradually.

Figure 7 illustrates the coefficient of friction for both the treated and untreated samples as a function of the testing duration.

It has been previously noted that DLC films exhibit a lower coefficient of friction than compound layers. Figure 7 corroborates this assertion, illustrating that the NIT and NITC samples possess a coefficient of friction closer to that of the base material, whereas the amorphous carbon films exhibit a significantly lower coefficient of friction than base material and the NIT and NITC samples.
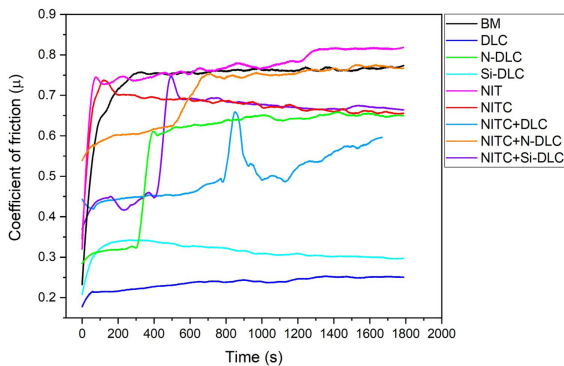
According to Bonetti et al.[11], one of the contributing factors to the low coefficient of friction exhibited by DLC films is the formation of a nanometric graphite layer between the DLC and its counterpart, which contributes to the wear of the film. The elevation in temperature within the contact region between the surfaces facilitates the release of hydrogen from the film, thereby promoting the formation of a graphite layer[11,66,67].

Consequently, the presence of hydrogen in diamond-like carbon (DLC) films is intricately linked to the coefficient of friction exhibited by the systems. Existing literature supports this mechanism by indicating that hydrogenated amorphous carbon films demonstrate a reduced coefficient of friction when compared to non-hydrogenated amorphous carbon films, commonly referred to as tetrahedral amorphous carbon (ta-C) films[68].

To complement the wear volume and coefficient of friction data, Table 5 delineates the depth of the craters following the tests, facilitating an analysis of the integrity of the films and layers post-testing.

Figure 6 illustrates a significant increase in the coefficient of friction of the N-DLC sample within this system, an observation that can be elucidated by the data presented in Table 5. The crater depth exceeded the thickness of the film, thereby suggesting that the film was entirely worn during the test, resulting in an elevated coefficient of friction. This sharp increase occurs at approximately 300 seconds, corresponding to a sliding distance of 63.1 meters. Upon examining Figure 6, it can be discerned that after the 63.1-meter sliding distance, the wear volume of the N-DLC film surpasses that of the other DLC films, reinforcing the interpretation of complete film wear.

Distinct behaviors have been observed in DLC and Si-DLC samples, which have not undergone complete wear during the testing procedures. This phenomenon arises from the film's thickness exceeding the crater depth, resulting in a relatively low coefficient of friction when compared to the other samples. Moreover, the Si-DLC exhibits intriguing characteristics as evidenced by its coefficient of friction (COF) curve depicted in Figure 7. While most samples demonstrate an increase in the coefficient of friction throughout the duration of the test, the Si-DLC reveals a notable decrease in the coefficient of friction. This observation aligns with previous findings regarding the stabilization of the film at elevated temperatures attributed to silicon doping[15,59].

Figure 7. Coefficient of friction of the treated and untreated material.

Table 5. Depth of craters in comparison with DLC films and nitrided/nitrocarburized layers thickness at the sliding distance of 378.2 m.

Treatment	Crater depth (μm)	Film thickness (μm)	Compound layer thickness (μm)	Total thickness (film + compound layer) (μm)
MB	26.54	-	-	-
NIT	8.81	-	3.11	3.11
NITC	5.60	-	2.15	2.15
DLC	2.66	5.51	-	5.51
N-DLC	3.18	3.05	-	3.05
Si-DLC	2.64	4.32	-	4.32
NITC+DLC	2.12	1.37	1.94	3.37
NITC+N-DLC	9.72	1.35	1.54	2.89
NITC+Si-DLC	2.05	3.40	3.33	6.73

In comparison with amorphous carbon film samples, the crater depth observed in NIT and NITC treatments was significantly more significant than the thickness of the compound layers. This phenomenon can be attributed to the debris released during the tests, which serves an abrasive function and adversely affects the tribological behavior of these layers. Nevertheless, despite the negative influence of the released debris on the wear resistance and coefficient of friction of the NIT and NITC samples, there is a notable enhancement in wear resistance when compared to the base material[60-63].

In reference to the coefficient of friction for samples NIT and NITC within this system, it can be observed that their values are comparable to those of the base material. This phenomenon can be attributed to the increased surface roughness resulting from plasma nitriding, in contrast to the smoother profiles of amorphous carbon films, which yield a higher coefficient of friction[18,68].

In the context of multilayer treatments such as NITC+DLC, NITC+N-DLC, and NITC+Si-DLC, a comparable coefficient of friction behavior to that of the N-DLC film is noted, wherein the coefficient of friction initially registers at lower levels and subsequently experiences a rapid increase, as illustrated in Figure 7. Furthermore, as indicated in Table 5, the crater depth is either greater than or approximately equal to the thickness of the amorphous carbon films. This alteration in crater depth impacts the coefficient of friction, as the structural integrity of the film is compromised, and the underlying compound layer beneath the DLC films may exert an influence on the testing results.

Consequently, the coefficient of friction for the multilayer treatments approaches that of the NIT and NITC samples at the conclusion of the examination, as these layers contribute significantly after the film has been extensively worn or is nearing complete degradation.

In the analysis of the morphology of the craters, as illustrated in Figure 8, various wear modes are observed, including grooving and rolling. These modes occur when abrasive particles slide across the surface of the sample and when the particles roll along the surface of the specimen during testing, respectively[63,69].

Martins et al.[56] identified craters featuring irregular edges on AISI M2 high-speed steel, specifically with polished and machined surfaces. According to the authors, these crater imperfections are referred to as ridgings, which arise from the insufficient penetration of abrasive particles in the central region. Numerous studies examining this wear test have associated these irregularities, particularly in non-coated samples.

The various modes may be associated with the characteristics of the coating being examined and the impact of the resultant coefficient of friction within the system. This is due to the grooving wear mode typically exhibiting a higher coefficient of friction, attributed to the limited number of particles present between the counter-body and the sample, which in turn generates a greater force on the surface[61,69,70].

It is noteworthy to observe in Figure 8B the existence of a mixed wear mode, which can be associated with the debris released from the nitrogen-doped diamond-like carbon (N-DLC) film. Initially, this debris contributed to the grooving wear mode; however, as the number of particles decreased, the prevalence of the grooving wear mode diminished. Furthermore, as the force exerted on the particles increased, the quantity of debris decreased[70].

Another significant observation is that in the samples exhibiting a higher coefficient of friction, the predominance of the grooving wear mode was evident. This result aligns with the extant literature, as the grooving wear mode is associated with a greater coefficient of friction in the system compared to the rolling wear mode[61,69,70].

Figure 9 illustrates the morphology of the craters corresponding to sample NITC+DLC for sliding distances of 126.1, 252.2, and 378.2 meters. Upon analysis of the images, the transition of wear modes is distinctly observable, commencing with the rolling wear mode when the Diamond-Like Carbon (DLC) film remains partially intact, immediately following the initial emergence of the nitrocarburizing layer, and progressing to the complete degradation of the film, culminating in the final formation of the compound layer.

This outcome is correlated with the coefficient of friction of the film, as illustrated in Figure 7, where a significant escalation in the coefficient of friction of the film is evident, attributed to the total wear of the film and the effects of the nitrocarburizing layer along with its grooving wear mode. However, upon examining Table 5, it is apparent that the
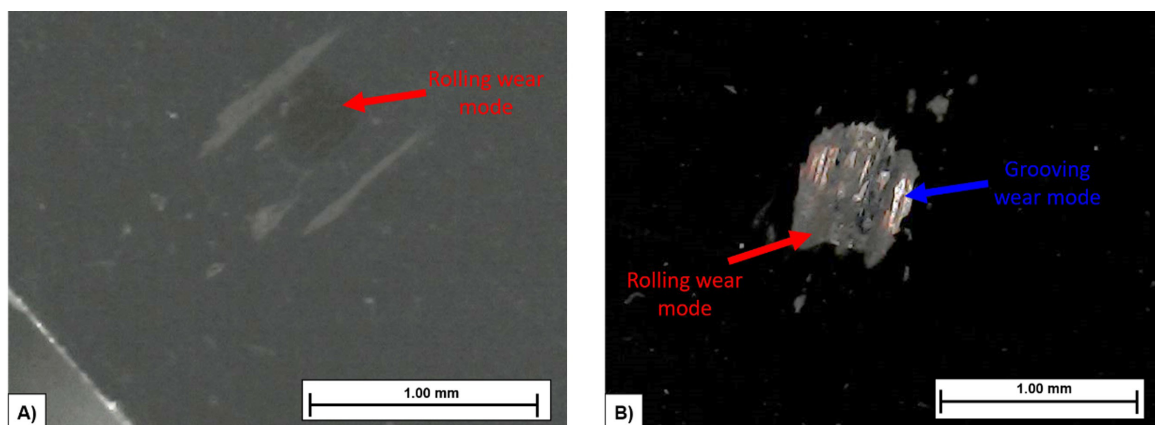
Figure 8. Crater morphology and wear modes of a) DLC film at the sliding distance of 126.1 m and b) N-DLC film at the sliding distance of 378.2 m.
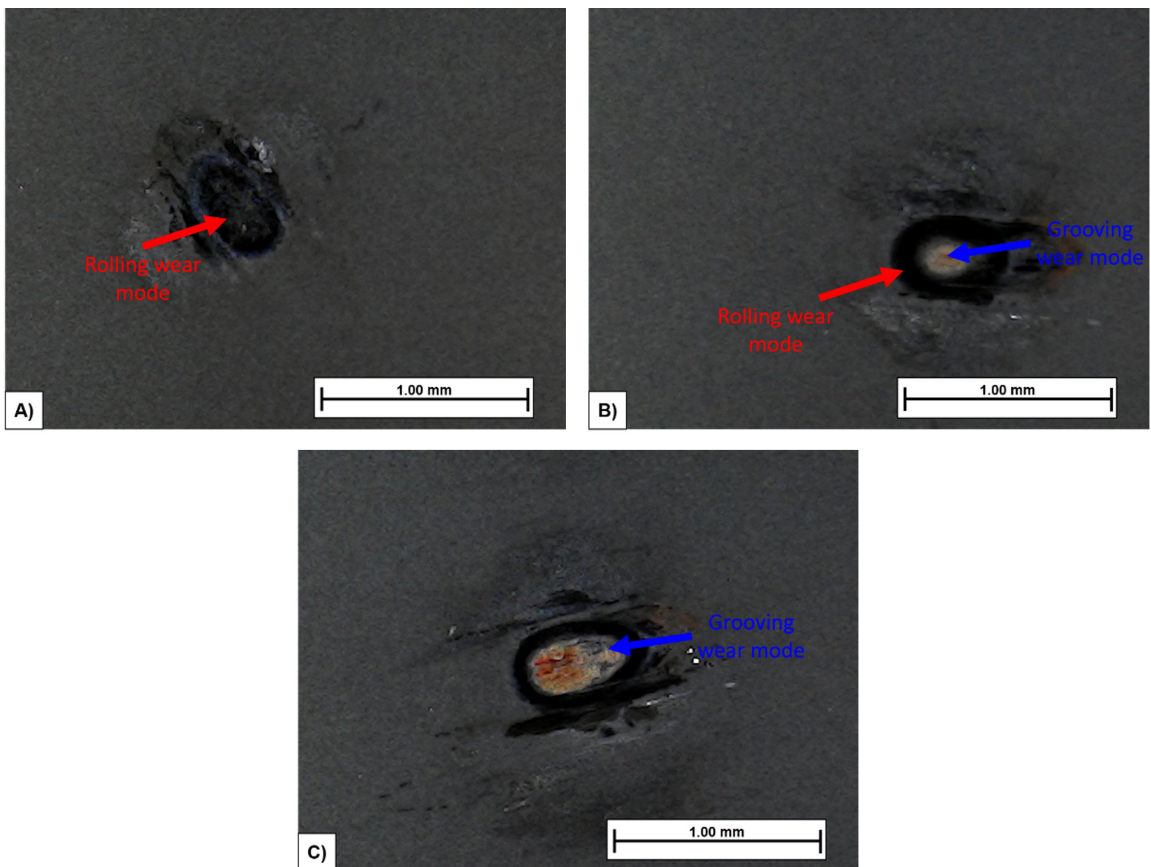
Figure 9. Morphology and wear modes of the NITC+DLC samples' craters at sliding distances of a) 126.1 m, b) 252.2 m, and c) 378.2 m.

film of the NITC+DLC sample has undergone complete wear. In contrast, the composite layer has maintained its integrity, a behavior that is also demonstrated in Figure 9.

4. Conclusions

This study examined the impact of duplex treatments, which combine nitrocarburizing with diamond-like carbon (DLC) coatings, on the wear resistance of AISI M2 steel. A cost-effective and less hazardous silicon precursor was successfully employed for doping. The integration of nitrogen and silicon modifies essential film properties, such as thickness, adhesion, wear resistance, and coefficient of friction, through alterations in the carbon bonding structure, the latter of which was validated using Raman spectroscopy.

Nitrocarburizing significantly enhanced both surface and subsurface hardness, and when combined with DLC or Si-DLC coatings, resulted in further improvements, especially in wear resistance. The Si-doped DLC applied over nitrocarburized substrates (NITC+Si-DLC) demonstrated the highest wear resistance. However, it did not achieve the lowest friction coefficient. The enhanced durability was ascribed to the synergistic effects of the hardened compound layer and the stabilization of sp^3 bonds within the Si-DLC film. Moreover, the investigation into the evolution of wear mechanisms and crater morphology during testing facilitated a deeper

comprehension of the multilayer system's tribological behavior. These findings contribute to the advancement of sophisticated multilayer coatings for cutting tools, with the objective of increasing the useful life under severe conditions.

5. Acknowledgments

6. References

1. Robertson J. Diamond-like amorphous carbon. Mater Sci Eng. 2002;37(4-6):129-281. http://doi.org/10.1016/S0927-796X(02)00005-0.

2. Cemin F, Boeira CD, Figueroa CA. On the understanding of the silicon-containing adhesion interlayer in DLC deposited on steel. Tribol Int. 2016;94:464-9. http://doi.org/10.1016/j.triboint.2015.09.044.

3. Almeida LS, Souza ARM, Costa LH, Rangel EC, Manfrinato MD, Rossino LS. Effect of nitrogen in the properties of diamond-like carbon (DLC) coating on Ti 6 Al 4 V substrate. Mater Res Express. 2020;7(6):065601. http://doi.org/10.1088/2053-1591/ab94fb.

4. Campos LAP, Almeida LS, Silva BP, Danelon MR, Aoki IV, Manfrinato MD, et al. Evaluation of nitriding, nitrocarburizing, organosilicon interlayer, diamond-like carbon film and duplex plasma treatment in the wear and corrosion resistance of AISI

4340 steel. J Mater Eng Perform. 2020;29(12):8107-21. http://doi.org/10.1007/s11665-020-05277-9.

5. Dalibón EL, Guitar MA, Trava-Airoldi V, Mücklich F, Brühl SP. Plasma nitriding and DLC coatings for corrosion protection of precipitation hardening stainless steel. Adv Eng Mater. 2016;18(5):826-32. http://doi.org/10.1002/adem.201500411.

6. Danelon MR, de Almeida LS, Manfrinato MD, Rossino LS. Study of the influence of a gradient gas flow as an alternative to improve the adhesion of Diamond-Like Carbon film in the wear and corrosion resistance on the nitrided AISI 4340 steel. Surf Interfaces. 2023;36:102352. http://doi.org/10.1016/j.surfin.2022.102352.

7. Tschiptschin AP. Duplex Coatings. In: Wang QJ, Chung YW, editors. Encyclopedia of Tribology. Boston: Springer US; 2013. p. 794-800. http://doi.org/10.1007/978-0-387-92897-5_694.

8. Almeida LS, Pereira MS, Antônio CA Jr, Silva FC, Prada Ramirez OM. Study of the effect of nitrogen on corrosion, wear resistance and adhesion properties of DLC films deposited on AISI 321H. Mater Res. 2022;25(Suppl 2):e20220141. http://doi.org/10.1590/1980-5373-MR-2022-0141.

9. Fayed SM, Chen D, Li S, Zhou Y, Wang H. Effect of bias voltage on characteristics of multilayer Si-DLC film coated on AA6061 aluminum alloy. J Mater Eng Perform. 2021;30(1):743-59. http://doi.org/10.1007/s11665-020-05397-2.

10. Sharifahmadian O, Mahboubi F, Yazdani S. Comparison between corrosion behaviour of DLC and N-DLC coatings deposited by DC-pulsed PACVD technique. Diamond Related Materials. 2019;95:60-70. http://doi.org/10.1016/j.diamond.2019.04.007.

11. Bonetti LF, Capote G, Santos LV, Corat EJ, Trava-Airoldi VJ. Adhesion studies of diamond-like carbon films deposited on Ti6Al4V substrate with a silicon interlayer. Thin Solid Films. 2006;515(1):375-9. http://doi.org/10.1016/j.tsf.2005.12.154.

12. Dalibon EL, Trava-Airoldi V, Pereira LA, Cabo A, Brühl SP. Wear resistance of nitrided and DLC coated PH stainless steel. Surf Coat Tech. 2014;255:22-7. http://doi.org/10.1016/j.surfcoat.2013.11.004.

13. Song Y, Han C, Zhen N, Wang Y, Leng Y, Wu Z, et al. Nitrogen-doped diamond-like carbon buffer layer enhances the mechanical and tribological properties of diamond-like carbon films deposited on nitrile rubber substrate. Coatings. 2024;14(4):515. http://doi.org/10.3390/coatings14040515.

14. Yang T, Xie M, Wang W, Wang C, Qi X, Deng Q, et al. Low friction and wear of Nitrogen-doped diamond-like carbon films deposited on NBR with different flows of N2 by DC-MS. Vacuum. 2024;220:112774. http://doi.org/10.1016/j.vacuum.2023.112774.

15. Wu W-J, Hon M-H. Thermal stability of diamond-like carbon films with added silicon. Surf Coat Tech. 1999;111(2-3):134-40. http://doi.org/10.1016/S0257-8972(98)00719-1.

16. Kim J-I, Jang Y-J, Kim J, Kim J. Effects of silicon doping on low-friction and high-hardness diamond-like carbon coating via filtered cathodic vacuum arc deposition. Sci Rep. 2021;11(1):3529. http://doi.org/10.1038/s41598-021-83158-4.

17. Vengudusamy B, Grafl A, Preinfalk K. Influence of silicon on the wear properties of amorphous carbon under dry and lubricated conditions. Tribol Lett. 2014;53(3):569-83. http://doi.org/10.1007/s11249-014-0295-2.

18. Ebrahimi M, Mahboubi F, Naimi-Jamal MR. Wear behavior of DLC film on plasma nitrocarburized AISI 4140 steel by pulsed DC PACVD: effect of nitrocarburizing temperature. Diamond Related Materials. 2015;52:32-7. http://doi.org/10.1016/j.diamond.2014.12.004.

19. Moreno-Barcenas A, Alvarado-Orozco JM, Carmona JMG, Mondragon-Rodriguez GC, Gonzalez-Hernandez J, Garcia-Garcia A. Synergistic effect of plasma nitriding and bias voltage on the adhesion of diamond-like carbon coatings on M2 steel by PECVD. Surf Coat Tech. 2018;374:327-37. http://doi.org/10.1016/j.surfcoat.2019.06.014.

20. Dalibon EL, Pecina JN, Cabo A, Trava-Airoldi VJ, Brühl SP. Fretting wear resistance of DLC hard coatings deposited on nitrided martensitic stainless steel. J Mater Res Technol. 2019;8(1):259-66. http://doi.org/10.1016/j.jmrt.2017.12.004.

21. Yetim AF, Kovacı H, Kasapoğlu AE, Bozkurt YB, Çelik A. Influences of Ti, Al and V metal doping on the structural, mechanical and tribological properties of DLC films. Diamond Related Materials. 2021;120:108639. http://doi.org/10.1016/j.diamond.2021.108639.

22. Berg JC. An introduction to interfaces and colloids. Singapore: World Scientific; 2009. http://doi.org/10.1142/7579.

23. Capote G, Silva GF, Trava-Airoldi VJ. Effect of hexane precursor diluted with argon on the adherent diamond-like properties of carbon films on steel surfaces. Thin Solid Films. 2015;589:286-91. http://doi.org/10.1016/j.tsf.2015.05.047.

24. Ghasemi MH, Ghasemi B, Semnani HRM. Wear performance of DLC coating on plasma nitrided Astaloy Mo. Diamond Related Materials. 2019;93:8-15. http://doi.org/10.1016/j.diamond.2019.01.016.

25. Barba E, Claver A, Montalà F, Palacio JF, Luis-Pérez CJ, Sala N, et al. Study of the industrial application of diamond-like carbon coatings deposited on advanced tool steels. Coatings. 2024;14(2):159. http://doi.org/10.3390/coatings14020159.

26. Wang X, Zhang X, Wang C, Lu Y, Hao J. High temperature tribology behavior of silicon and nitrogen doped hydrogenated diamond-like carbon (DLC) coatings. Tribol Int. 2022;175:107845. http://doi.org/10.1016/j.triboint.2022.107845.

27. Nass KCF, Radi PA, Leite DMG, Massi M, da Silva Sobrinho AS, Dutra RCL, et al. Tribomechanical and structural properties of a-SiC:H films deposited using liquid precursors on titanium alloy. Surf Coat Tech. 2015;284:240-6. http://doi.org/10.1016/j.surfcoat.2015.06.080.

28. Materne T, de Buyl F, Witucki GL. Organosilane technology in coating applications: review and perspective. Midland: Dow Corning Corp; 2012.

29. Casiraghi C, Ferrari AC, Robertson J. Raman spectroscopy of hydrogenated amorphous carbons. Phys Rev B Condens Matter Mater Phys. 2005;72(8):085401. http://doi.org/10.1103/PhysRevB.72.085401.

30. Singha A, Ghosh A, Roy A, Ray NR. Quantitative analysis of hydrogenated diamondlike carbon films by visible Raman spectroscopy. J Appl Phys. 2006;100(4):044910. http://doi.org/10.1063/1.2219983.

31. Vidakis N, Antoniadis A, Bilalis N. The VDI 3198 indentation test evaluation of a reliable qualitative control for layered compounds. J Mater Process Technol. 2003;143-144:481-5. http://doi.org/10.1016/S0924-0136(03)00300-5.

32. Rutherford KL, Hutchings IM. A micro-abrasive wear test, with particular application to coated systems. Surf Coat Tech. 1996;79(1-3):231-9. http://doi.org/10.1016/0257-8972(95)02461-1.

33. Martins PS, Carneiro JRG, Ba ECT, Vieira VF, Amaral DB, Cruz NC. Study on the tribological behavior of wear and friction coefficient on AISI M35 high-speed steel with and without DLC coating. Mater Res. 2022;25:e20200577. http://doi.org/10.1590/1980-5373-mr-2020-0577.

34. Gonzalez-Carmona JM, Mondragon-Rodriguez GC, Galvan-Chaire JE, Gomez-Ovalle AE, Caceres-Diaz LA, Gonzalez-Hernandez J, et al. Plasma-assisted nitriding of M2 tool steel: An experimental and theoretical approach. ArXiv. 2018 [cited 2024 Dec 4]. Available from: http://arxiv.org/abs/1810.06593. Pre Print.

35. Lampe T, Eisenberg S, Laudien G. Compound layer formation during plasma nitriding and plasma nitrocarburising. Surf Eng. 1993;9(1):69-76. http://doi.org/10.1179/sur.1993.9.1.69.

36. Franceschini DF. Plasma-deposited a-C(N): H films. Braz J Phys. 2000;30(3):517-26. http://doi.org/10.1590/S0103-97332000000300007.

37. Long J, Nand A, Ray S. Application of spectroscopy in additive manufacturing. Materials. 2021;14(1):203. http://doi.org/10.3390/ma14010203.

38. Ba ECT, Dumont MR, Martins PS, Pinheiro BS, Cruz MPM, Barbosa JW. Deconvolution process approach in Raman spectra

of DLC coating to determine the sp³ hybridization content using the ID/IG ratio in relation to the quantification determined by X-ray photoelectron spectroscopy. Diamond Related Materials. 2022;122:108818. http://doi.org/10.1016/j.diamond.2021.108818.

39. Ferrari AC, Robertson J. Interpretation of Raman spectra of disordered and amorphous carbon. Phys Rev B Condens Matter Mater Phys. 2000;61(20):14095-107. http://doi.org/10.1103/PhysRevB.61.14095.

40. Cemin F, Bim LT, Menezes CM, Costa MEHM, Baumvol IJR, Alvarez F, et al. The influence of different silicon adhesion interlayers on the tribological behavior of DLC thin films deposited on steel by EC-PECVD. Surf Coat Tech. 2015;283:115-21. http://doi.org/10.1016/j.surfcoat.2015.10.031.

41. Choi J, Nakao S, Miyagawa S, Ikeyama M, Miyagawa Y. The effects of Si incorporation on the thermal and tribological properties of DLC films deposited by PBII&D with bipolar pulses. Surf Coat Tech. 2007;201(19-20):8357-61. http://doi.org/10.1016/j.surfcoat.2006.02.084.

42. Cui WG, Lai QB, Zhang L, Wang FM. Quantitative measurements of sp³ content in DLC films with Raman spectroscopy. Surf Coat Tech. 2010;205(7):1995-9. http://doi.org/10.1016/j.surfcoat.2010.08.093.

43. Ţucureanu V, Matei A, Avram AM. FTIR spectroscopy for carbon family study. Crit Rev Anal Chem. 2016;46(6):502-20. http://doi.org/10.1080/10408347.2016.1157013.

44. Safari R, Sohbatzadeh F, Mohsenpour T. Optical and electrical properties of N-DLC films deposited by atmospheric pressure DBD plasma: effect of deposition time. Surf Interfaces. 2020;21:100795. http://doi.org/10.1016/j.surfin.2020.100795.

45. Brunatto SF. Nitretação por plasma de ferro sinterizado [dissertation]. Florianópolis: Universidade Federal de Santa Catarina; 1993.

46. Damin KVS. Tratamentos Termoquímicos sequenciais por plasma do aço AISI 1005 [dissertation]. Florianópolis: Universidade Federal de Santa Catarina; 2015.

47. Silva HRT. Estudo do processo de nitrocementação por plasma [thesis]. Florianópolis: Universidade Federal de Santa Catarina; 2003.

48. Rocha AS. Influência do estado superficial prévio na nitretação a plasma do aço AISI M2 [thesis]. Porto Alegre: Universidade Federal do Rio Grande do Sul; 2000.

49. Tier MAD. Avaliação da resistência ao desgaste do aço AISI M2 nitretado a plasma [thesis]. Porto Alegre: Universidade Federal do Rio Grande do Sul; 1998.

50. Sousa R, Costa TC, Costa J, Santos F, Nascimento I, Souza I, et al. Cathodic cage plasma deposition of DLC film on D2 steel substrate. J Mater Sci. 2019;7:17-22.

51. Basso RLO, Figueroa CA, Zagonel LF, Pastore HO, Wisnivesky D, Alvarez F. Effect of carbon on the compound layer properties of AISI H13 tool steel in pulsed plasma nitrocarburizing. Plasma Process Polym. 2007;4(S1):S728-31. http://doi.org/10.1002/ppap.200731806.

52. Fontes MA, Scheid VHB, Machado DS, Casteletti LC, Nascente PAP. Morphology of the DIN 100Cr6 Case hardened steel after plasma nitrocarburizing process. Mater Res. 2019;22(3):1-6. http://doi.org/10.1590/1980-5373-mr-2018-0612.

53. Zagonel LF, Figueroa CA, Droppa R Jr, Alvarez F. Influence of the process temperature on the steel microstructure and hardening in pulsed plasma nitriding. Surf Coat Tech. 2006;201(1-2):452-7. http://doi.org/10.1016/j.surfcoat.2005.11.137.

54. Imai T, Harigai T, Tanimoto T, Isono R, Iijima Y, Suda Y, et al. Hydrogen-free fluorinated DLC films with high hardness prepared by using T-shape filtered arc deposition system. Vacuum. 2019;167:536-41. http://doi.org/10.1016/j.vacuum.2018.07.009.

55. Zhao Y, Xu F, Xu J, Li D, Sun S, Gao C, et al. Effect of the bias-graded increment on the tribological and electrochemical corrosion properties of DLC films. Diamond Related Materials. 2022;130:109421. http://doi.org/10.1016/j.diamond.2022.109421.

56. Martins PS, Pires SS, Silva ER, Vieira VF, Talibouya Ba EC, Rodrigues Dias CA. Tribological aspects of the Diamond-like carbon film applied to different surfaces of AISI M2 steel. Wear. 2022;506–507:204469. http://doi.org/10.1016/j.wear.2022.204469.

57. Danelon MR, Soares F, Manfrinato MD, Rossino LS. Estudo do efeito da nitretação iônica a plasma na resistência ao desgaste do aço SAE 1020 utilizado em matriz de conformação. Rev Bras Apl Vácuo. 2020;39(2):142. http://doi.org/10.17563/rbav.v39i2.1166.

58. Conde FF, Diaz JAÁ, Silva GF, Tschiptschin AP. Dependence of wear and mechanical behavior of Nitrocarburized/CrN/DLC layer on film thickness. Mater Res. 2019;22(2):e20180499. http://doi.org/10.1590/1980-5373-mr-2018-0499.

59. Kolawole FO, Kolawole SK, Varela LB, Owa AF, Ramirez MA, Tschiptschin AP. Diamond-Like Carbon (DLC) coatings for automobile applications. In: Mallik A, editor. Engineering applications of diamond. London: IntechOpen; 2021. http://doi.org/10.5772/intechopen.95063.

60. Almeida EAS, Costa CE, Milan JCG. Study of the nitrided layer obtained by different nitriding methods. Materia. 2015;20(2):460-5. http://doi.org/10.1590/S1517-707620150002.0046.

61. Cozza RC, Tanaka DK, Souza RM. Friction coefficient and abrasive wear modes in ball-cratering tests conducted at constant normal force and constant pressure: preliminary results. Wear. 2009;267(1-4):61-70. http://doi.org/10.1016/j.wear.2009.01.055.

62. Duman K, Karabeyoğlu SS, Yaman P. Effect of nitriding conditions and operation temperatures on dry sliding wear properties of the aluminum extrusion die steel in the industry. Mater Today Commun. 2022;31:103628. http://doi.org/10.1016/j.mtcomm.2022.103628.

63. Mergler YJ, Huis in 't Veld AJ. Micro-abrasive wear of semi-crystalline polymers. Tribology Series. 2003;41:165-73. https://doi.org/10.1016/S0167-8922(03)80129-3.

64. Cozza RC. Estudo do comportamento do coeficiente de desgaste e dos modos de desgaste abrasivo em ensaios de desgaste micro-abrasivo [thesis]. São Paulo: Escola Politécnica da Universidade de São Paulo; 2006. http://doi.org/10.11606/D.3.2006.tde-31032008-101929.

65. Donnet C, Grill A. Friction control of diamond-like carbon coatings. Surf Coat Tech. 1997;94-95:456-62. http://doi.org/10.1016/S0257-8972(97)00275-2.

66. Skonieski AFO. Desenvolvimento de superfícies com filmes de "Diamond-Like Carbon" com adesão melhorada e baixo coeficiente de atrito aplicáveis em conformação mecânica [thesis]. Porto Alegre: Universidade Federal do Rio Grande do Sul; 2013.

67. Erdemir A, Eryilmaz OL, Kim SH. Effect of tribochemistry on lubricity of DLC films in hydrogen. Surf Coat Tech. 2014;257:241-6. http://doi.org/10.1016/j.surfcoat.2014.08.002.

68. Heydarzadeh Sohi M, Ebrahimi M, Honarbakhsh Raouf A, Mahboubi F. Effect of plasma nitrocarburizing temperature on the wear behavior of AISI 4140 steel. Surf Coat Tech. 2010;205:S84-9. http://doi.org/10.1016/j.surfcoat.2010.04.054.

69. Cozza RC. Third abrasive wear mode: is it possible? J Mater Res Technol. 2014;3(2):191-3. http://doi.org/10.1016/j.jmrt.2014.03.010.

70. Kusano Y, Hutchings IM. Sources of variability in the free-ball micro-scale abrasion test. Wear. 2005;258(1-4):313-7. http://doi.org/10.1016/j.wear.2004.02.020.

Data Availability

The entire dataset supporting the results of this study was published in the article itself.